^{1}H NMR Study of the Reduced Cytochrome *c*′ from *Rhodopseudomonas palustris* Containing a High-Spin Iron(II) Heme Moiety

Ivano Bertini,*,† Alexander Dikiy,† Claudio Luchinat,‡ Riccardo Macinai,† and Maria Silvia Viezzoli†

Department of Chemistry, University of Florence, Via Gino Capponi 7, 50121 Florence, Italy, and Department of Soil Science and Plant Nutrition, University of Florence, P. le delle Cascine 28, 50144 Florence, Italy

Received May 12, 1998

The assignment of the hyperfine shifted signals of the reduced cytochrome *c*′ from *Rhodopseudomonas palustris* has been obtained through saturation transfer experiments with assigned signals of the high-spin oxidized protein and through tailored experiments to reveal proton−proton dipolar connectivities in paramagnetic molecules. The peculiar shift pattern consisting of the 1-, 8-, and 5-methyl signals shifted upfield and the 3-methyl signal downfield, which is shared by all cytochromes *c*′ so far described, has been semiquantitatively related to the orientation of the histidine plane with respect to the iron−heme nitrogen axes. The research is meaningful with respect to the use of paramagnetic NMR as a tool to obtain direct structural information on all high spin iron(II) heme containing systems, including deoxyglobins.

Introduction

^{1}H NMR (nuclear magnetic resonance) spectroscopy is useful for obtaining local structural information in paramagnetic systems. A simple glance at the ^{1}H NMR spectrum, and sometimes at more than one spectrum, may provide information on the groups bound to the paramagnetic metal ion. Histidines, for example, can be recognized from the proton signal pattern and from NH/ND exchangeability in D_2O,[1] the spectrum of Glu CH_2's can be informative on the type of binding,[2] and so on. In heme proteins consistent progress has been made with high spin Fe^{3+} containing oxidized proteins.[3] The ion contains five unpaired electrons, i.e., one per orbital. The proton hyperfine shifts in the heme ligand largely arise from the delocalization of unpaired electrons through σ bonds, which involves the $d_{x^2-y^2}$ metal ion orbital[4] (Scheme 1A). All of the peripheral CH_3 and CH_2 protons of the heme are shifted several tens of ppm downfield. The temperature dependence of the shifts provides information on the ZFS parameters of the largely $S = {}^5/_2$ ground state.[5]

In low spin Fe^{3+} containing systems, the unpaired electron can occupy the d_{xz} or the d_{yz} orbital, both of which are degenerate in D_{4h} symmetry (Scheme 1B),[6,7] or more unlikely, the d_{xy} orbital (Scheme 1C).[8−10] The former is the situation which is always encountered in cytochromes and other biological molecules. When an axial ligand, like histidine, breaks the axial symmetry (Scheme 1B) through its π bond, two inequivalent orbitals are obtained out of d_{xz} and d_{yz}. Therefore the unpaired electron resides in the one which is involved with the π orbital of the imidazole ring.[11,12] Depending on the orbital occupancy, the shift pattern changes dramatically;[12−14] in turn, the orbital occupancy depends on the orientation of the imidazole plane.[15] If two imidazoles or one imidazole and a methionine are the axial ligands, the effects are simply additive.[12]

The problem has not yet been addressed for high spin Fe^{2+} containing systems with $S = 2$. In these systems the shift is smaller than in high spin $S = {}^5/_2$ containing systems,[16,17] and not only for the spin value but also for the fact that the large Fe^{2+} ion is out of the heme plane, thus reducing the σ spin delocalization.[18,19] In the presence of large Curie relaxation[20,21] due to the large magnetic moment and low rotational correlation time, the heme signals are broad and not much shifted. Large

† Department of Chemistry.
‡ Department of Soil Science and Plant Nutrition.

(1) Bertini, I.; Canti, G.; Luchinat, C.; Mani, F. *J. Am. Chem. Soc.* **1981**, *103*, 7784.
(2) Maroney, M. J.; Kurtz, D. M., Jr.; Nocek, J. M.; Pearce, L. L.; Que, L., Jr. *J. Am. Chem. Soc.* **1986**, *108*, 6871.
(3) Clark, K.; Dugad, L. B.; Bartsch, R. G.; Cusanovich, M. A.; La Mar, G. N. *J. Am. Chem. Soc.* **1996**, *118*, 4654.
(4) Budd, D. L.; La Mar, G. N.; Langry, K. C.; Smith, K. M.; Nayyir-Mazhir, R. *J. Am. Chem. Soc.* **1979**, *101*, 6091.
(5) La Mar, G. N.; Walker, F. A. *J. Am. Chem. Soc.* **1973**, *95*, 6950.
(6) Zerner, M.; Gouterman, M.; Kobayashi, H. *Theor. Chem. Acta* **1966**, *6*, 363.
(7) Loew, G. H. In *Iron Porphyrins*; Lever, A. B. P., Gray, H. B., Eds.; Addison-Wesley: Reading, MA, 1983; pp 1−88.
(8) Safo, M. K.; Gupta, G. P.; Watson, C. T.; Simonis, U.; Walker, F. A.; Scheidt, W. R. *J. Am. Chem. Soc.* **1992**, *114*, 7066.
(9) Walker, F. A.; Nasri, H.; Turowska-Tyrk, I.; Mohanrao, K.; Watson, C. T.; Shokhirev, N. V.; Debrunner, P. G.; Scheidt, W. R. *J. Am. Chem. Soc.* **1996**, *118*, 12109.
(10) Wolowiec, S.; Latos-Grazynski, L.; Mazzanti, M.; Marchon, J.-S. *Inorg. Chem.* **1997**, *36*, 5761.
(11) Feng, Y. Q.; Roder, H.; Englander, S. W. *Biophys. J.* **1990**, *57*, 15.
(12) Turner, D. L.; Williams, R. J. P. *Eur. J. Biochem.* **1993**, *211*, 555.
(13) Wüthrich, K. *Struct. Bonding* **1970**, *8*, 53.
(14) Shokhirev, N. V.; Shokhireva, T. K.; Polam, J. R.; Watson, C. T.; Raffii, K.; Simonis, U.; Walker, F. A. *J. Phys. Chem.* **1997**, *101*, 2778.
(15) Bertini, I.; Turano, P.; Vila, A. J. *Chem. Rev.* **1993**, *93*, 2833.
(16) La Mar, G. N.; Walker, F. A. In *The Porphyrins*; Dolphin, D. Ed.; Academic Press: New York, 1979; pp 61−157.
(17) Bertini, I.; Luchinat, C. *NMR of paramagnetic molecules in biological systems*; Benjamin/Cummings: Menlo Park, CA, 1986.
(18) Jameson, G. B.; Molinaro, F. S.; Ibers, J. A.; Collman, J. P.; Brauman, J. I.; Rose, E.; Suslick, K. S. *J. Am. Chem. Soc.* **1978**, *100*, 6769.
(19) Jameson, G. B.; Molinaro, F. S.; Ibers, J. A.; Collman, J. P.; Brauman, J. I.; Rose, E.; Suslick, K. S. *J. Am. Chem. Soc.* **1980**, *102*, 3224.
(20) Gueron, M. *J. Magn. Reson.* **1975**, *19*, 58.
(21) Vega, A. J.; Fiat, D. *Mol. Phys.* **1976**, *31*, 347.

S0020-1669(98)00531-X CCC: $15.00
Published on Web 09/01/1998

Scheme 1

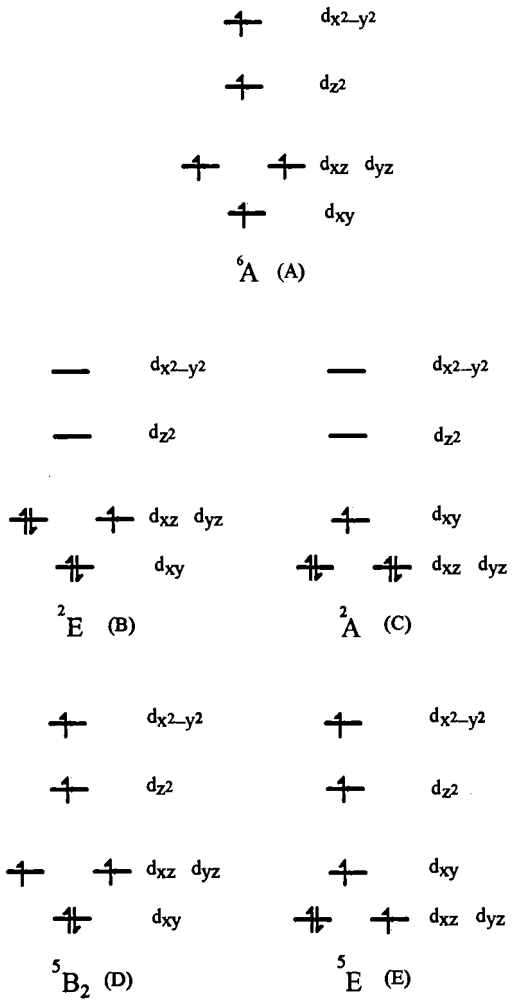

line widths and small hyperfine shifts are the worst characteristics for a successful interpretation of the ^{1}H NMR spectra.

We address here the problem of the shift pattern in reduced cytochromes *c′* by taking the opportunity to study the monomeric form of the isoprotein from *Rhodopseudomonas palustris*. Cytochromes *c′* contain a five-coordinated heme iron and are devoted to electron transfer.[22] The iron ion is bound to the heme moiety and to an apical histidine[23−27] which has a pK_a of about 9.[28,29] In the resting state below pH 9, the protein contains Fe^{3+}, which can be reduced to Fe^{2+} with dithionite. The latter species has been studied in the dimeric cyt *c′* from *Rhodocyclus gelatinosus*, and an extensive assignment of the hyperfine shift has been obtained.[30] In both the latter and the present

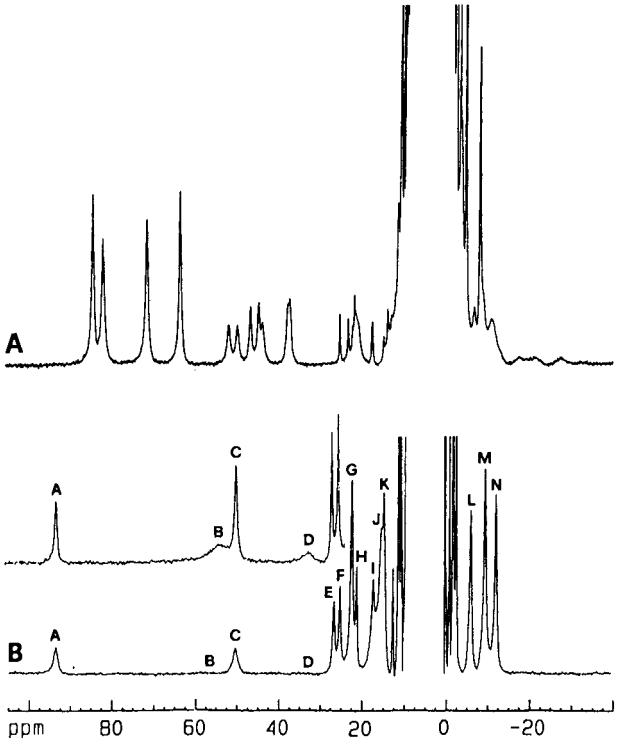

Figure 1. ^{1}H NMR spectra (298 K, 600 MHz) of the oxidized (A) and reduced (B) forms of the cytochrome *c′* from *R. palustris* in 100 mM phosphate buffer pH 4.9 in water solution.. The inset in B shows the downfield region of the spectrum recorded at 200 MHz.

cytochrome *c′*, the heme methyls 1-, 5-, and 8-CH_3 are shifted upfield and 3-CH_3 is shifted downfield. This is a quite unusual pattern. In light of the recent X-ray structure of *R. gelatinosus* cytochrome *c′*, a possible explanation is here provided which links the shift pattern to the orientation of the imidazole plane with respect to the Fe−heme nitrogen directions. This explanation is consistent with available X-ray and NMR data on reduced deoxyglobins and is proposed as a spectroscopic criterion for all high-spin ferrohemes, with an apical histidine ligand.

Experimental Section

All chemicals used were of the best quality available. The protein was purified in the oxidized form as described earlier.[31] Reduction of the protein was achieved by addition of sodium dithionite to the protein solution.

Samples for NMR spectroscopy (about 3 mM protein) were prepared in 100 mM phosphate buffer (either in H_2O or D_2O), pH 4.9.

The NMR spectra were recorded on AMX 600 and MSL 200 Bruker spectrometers operating at 600.14 and 200.13 MHz Larmor frequencies, respectively. The spectra were calibrated by assigning the water (or residual water) signal at 298 K a shift from TMS of 4.81 ppm.

Longitudinal relaxation rates were measured using a nonselective inversion recovery pulse sequence.[32] The T_1 values were obtained from a two-parameter fit of the data to an exponential recovery function.[33]

1D NOE (nuclear Overhauser effect) spectra were recorded in the difference mode using previously described acquisition schemes.[33,34] Recycle delays and irradiation times ranged from 170 to 250 and from 75 to 130 ms, respectively.

(22) Pettigrew, G. W.; Moore, G. R. *Cytochromes c; Biological Aspects*; Springer-Verlag: Berlin, 1987.
(23) Weber, P. C.; Bartsch, R. G.; Cusanovich, M. A.; Hamlin, R. C.; Howard, A.; Jordan, S. R.; Kamen, M. D.; Meyer, T. E.; Weatherford, D. W.; Xuong, N.-H.; Salemme, F. R. *Nature* **1980**, *286*, 302.
(24) Weber, P. C.; Howard, A.; Xuong, N.-H.; Salemme, F. R. *J. Mol. Biol.* **1981**, *153*, 399.
(25) Yasui, M.; Harada, S.; Kai, Y.; Kasai, N.; Kusunoki, M.; Matsuura, Y. *J. Biochem.* **1992**, *111*, 302.
(26) Ren, Z.; Meyer, T. E.; McRee, D. E. *J. Mol. Biol.* **1993**, *234*, 433.
(27) Archer, M.; Banci, L.; Dikaya, E.; Romao, M. J. *JBIC* **1997**, *2*, 611.
(28) La Mar, G. N.; Jackson, J. T.; Dugad, L. B.; Cusanovich, M. A.; Bartsch, R. G. *J. Biol. Chem.* **1990**, *265*, 16173.
(29) Banci, L.; Bertini, I.; Turano, P.; Vicens Oliver, M. *Eur. J. Biochem.* **1992**, *204*, 107.
(30) Bertini, I.; Gori, G.; Luchinat, C.; Vila, A. J. *Biochemistry* **1993**, *32*, 776.
(31) Bartsch, R. G. *Methods Enzymol.* **1971**, *23*, 344.
(32) Vold, R. L.; Waugh, J. S.; Klein, M. P.; Phelps, D. E. *J. Chem. Phys.* **1968**, *48*, 3831.
(33) Bertini, I.; Luchinat, C. *NMR of paramagnetic substances*; Coord. Chem. Rev. 150; Elsevier: Amsterdam, 1996; pp 1−300.
(34) Banci, L.; Bertini, I.; Luchinat, C.; Piccioli, M.; Scozzafava, A.; Turano, P. *Inorg. Chem.* **1989**, *28*, 4650.

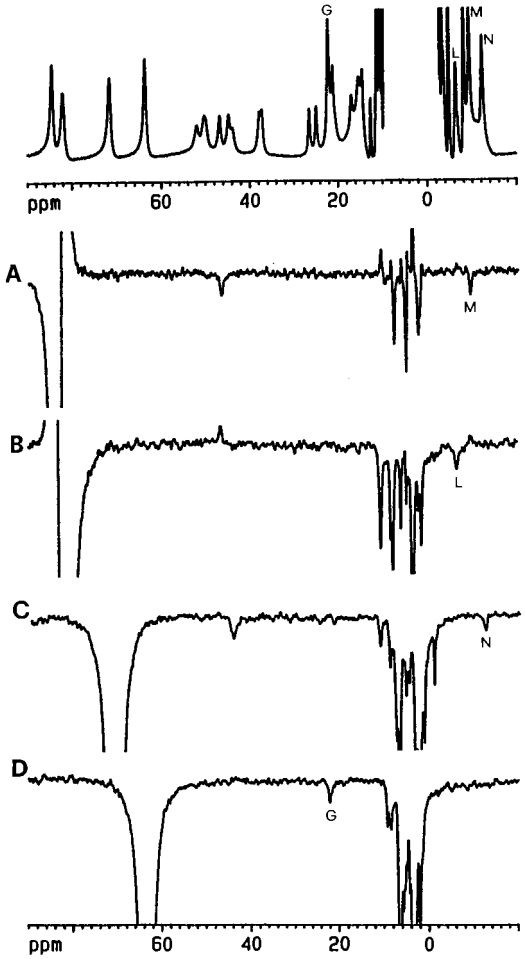

Figure 2. NMR spectra (298 K, 600 MHz) of a 100 mM phosphate buffer D_2O solution at pH 4.9 of cytochrome *c*′ from *R. palustris* containing about equal amounts of the reduced and oxidized species. The upper trace shows the reference spectrum. 1D NOE difference spectra obtained upon saturation of the heme methyl signals of the oxidized form are shown in the other traces: (A) 8-CH_3, (B) 1-CH_3, (C) 5-CH_3, (D) 3-CH_3.

1D saturation experiments were performed in a way analogous to 1D NOE experiments on the sample containing about an equal quantity of the reduced and oxidized protein forms.

2D NOESY[35] (nuclear Overhauser spectroscopy) and SuperWeft NOESY[36] experiments were recorded in the phase-sensitive mode at 293 and 298 K. The latter resulted in effective suppression of the dipolar connectivities between protons located far away from the paramagnetic center. Spectra were acquired with 512 points in the f_1 dimension, from 128 to 256 scans per experiment, and 2K data points in the f_2 dimension. The mixing times were 35 or 55 ms. The data matrices were multiplied by a cosine squared window function in both dimensions, prior to Fourier transformation.

The standard Bruker software package was used for data processing.

Results

The 298 K, 600 MHz ^{1}H NMR spectra of the oxidized and reduced forms of cytochrome *c*′ from *R. palustris* are shown in Figure 1, traces A and B, respectively. Both spectra reveal several hyperfine shifted signals, due to the paramagnetic nature of both species. An extensive assignment of the protons close to the iron ion in the oxidized form of cytochrome *c*′ from *R. palustris* has been reported recently by La Mar and co-workers.[3]

(35) Macura, S.; Ernst, R. R. *Mol. Phys.* **1980**, *41*, 95.
(36) Chen, Z. G.; de Ropp, J. S.; Hernandez, G.; La Mar, G. N. *J. Am. Chem. Soc.* **1994**, *116*, 8772−8783.

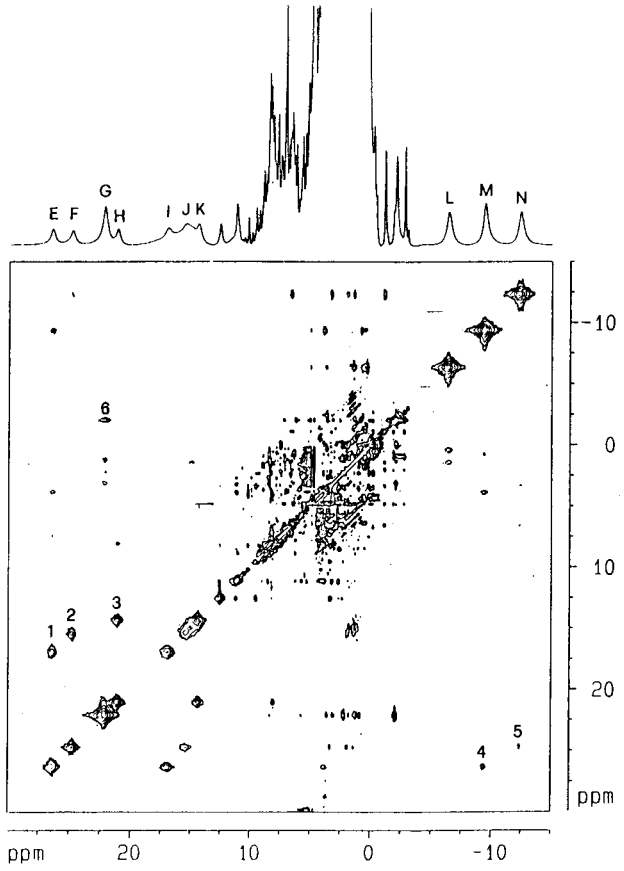

Figure 3. 2D NOESY spectrum (298 K, 600 MHz) of the reduced cytochrome *c*′ from *R. palustris* in 100 mM phosphate buffer D_2O solution at pH 4.9. The cross-peak assignment is as follows: (1) 7Hα−7Hα′; (2) 6-Hα−6Hα′; (3) Hβ−Hβ′ His; (4) 8-CH_3−7Hα; (5) 5-CH_3−6Hα; (6) 3-CH_3−4-$C_\beta H_3$.

Since the present cytochrome *c*′ has been purified from a strain different from that used earlier, we performed an independent assignment of the heme protons of the oxidized form. The obtained assignment is in complete agreement with the previous one. As the strategy used to assign the hyperfine shifted signals was similar to that published by La Mar et al.;[3] we will omit the details concerning the assignment of the oxidized form.

To proceed with an assignment of the reduced species, we took advantage of the assignment of the oxidized form. The spectrum of a sample containing about equal quantities of the reduced and oxidized forms of the protein, together with 1D saturation transfer spectra obtained by saturation of the methyl proton signals of the oxidized form, is presented in Figure 2. The simultaneous observation of the signals corresponding to the reduced and oxidized species indicates that the exchange rate between the reduced and oxidized species is slow on the NMR time scale ($\tau^{-1} < 2 \times 10^4$ rad s^{-1}). The saturation transfer experiments allowed us to unambiguously set the correspondences between the ^{1}H NMR signals in the reduced and oxidized forms. As follows from the saturation transfer experiments, signals G, L, M, and N correspond to the 3-, 1-, 8-, and 5-CH_3 heme signals, respectively.

Once the assignment of the methyl NMR signals of the reduced species was obtained, we proceeded with the assignment of other heme resonances through SuperWeft NOESY experiments.[36] A 2D NOESY spectrum of the reduced protein in the 30 to −15 ppm region is shown in Figure 3. The dipolar connectivities of the 5- and 8-CH_3 (signals N and M) with downfield signals F and E (cross peaks 5 and 4), respectively,

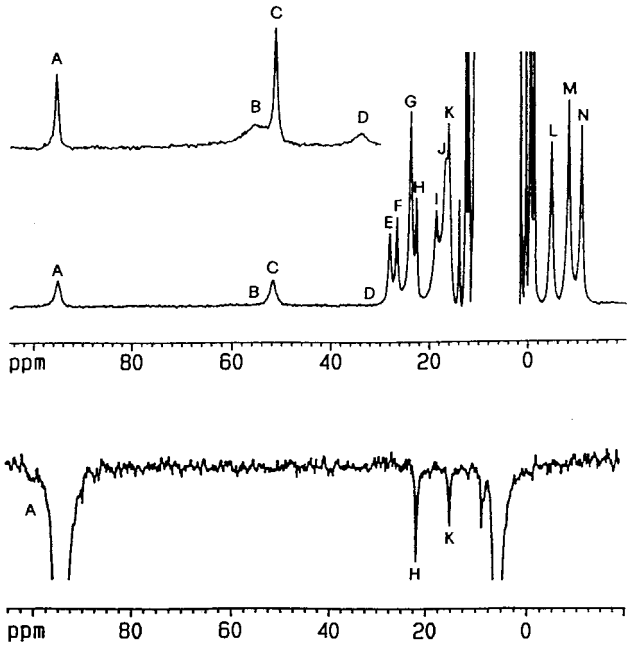

Figure 4. Spectra (298 K, 600 MHz) of the reduced cytochrome *c′* from *R. palustris* in 100 mM phosphate buffer water solution at pH 4.9. The upper trace shows the reference spectrum. The lower trace shows the 1D NOE spectrum obtained upon saturation of signal A. The inset shows the downfield region of the spectrum recorded at 200 MHz.

Table 1. Chemical Shift Data and T_1 Values of the Hyperfine Shifted Signals of the Reduced Cytochrome *c′* from *R. palustris* at 298 K

signal	chem shift, ppm	T_1, ms	assignment
A	93.74	6.0 ± 0.5^a	NHδ His
B	53.73	$<1.5^a$	Hδ2 His
C	49.70	12.2 ± 0.4^a	?
D	32.01	$<1.5^a$	Hϵ1 His
E	26.36	48.8 ± 5.1^b	7-Hα
F	24.76	54.9 ± 3.4^b	6-Hα
G	22.10	46.3 ± 3.3^b	3-CH_3
H	21.08	52.3 ± 2.6^b	Hβ His
I	16.92	28.8 ± 1.7^b	7-Hα'
J	15.36	21.5 ± 1.6^b	6-Hα'
K	14.37	38.7 ± 2.1^b	Hβ' His
L	−6.38	64.7 ± 2.0^b	1-CH_3
M	−9.38	54.5 ± 2.9^b	8-CH_3
N	−12.36	55.2 ± 3.2^b	5-CH_3

[a] Measured at 200 MHz. [b] Measured at 600 MHz.

and the strong cross peaks of the latter signals with signals J and I (cross peaks 2 and 1), allowed us to assign signals of 6-Hα and 7-Hα geminal protons. Signals H and K giving rise to cross peak 3 have been assigned as due to H_β geminal protons of the histidine coordinated to the iron ion in analogy with cytochrome *c′* from *R. gelatinosus*.[30] The intense connectivity of the 3-CH_3 signal (signal G) with a signal of intensity 3 at −2.76 ppm (cross peak 6) sets the latter signal as due to the thioether 4-$C_\beta H_3$.

When the spectrum of the reduced protein is recorded in water solution, a new signal (signal A) with respect to the analogous spectrum in D_2O is observed at 93.74 ppm (Figure 1B). The exchangeable nature of this signal, together with the large hyperfine shift and short longitudinal relaxation time, indicates that this is the NH ring proton of the coordinated histidine. A 1D NOE spectrum obtained by saturating signal A is reported in Figure 4. The observation of NOEs on signals H and K, earlier assigned as due to Hβ' protons of the histidine, allows us to unambiguously assign signal A as due to the NHδ ring proton of the proximal histidine. Two additional broad signals (signals B and D), which were not observed at 600 MHz, are observed in the spectrum recorded at 200 MHz. The spectrum of the protein in water solution acquired at 200 MHz is shown in the insets of Figures 1B and 4. Both longitudinal and transverse relaxation times of signals B and D indicate that most probably these signals are due to Hδ1 and Hϵ1 histidine ring protons, which are the closest ones to the iron ion. Indeed, this assignment has been confirmed through 1D NOE experiments. Upon saturation of signal D we observed a NOE on signal A (data not shown), while no NOE on strongly downfield shifted signals is observed by saturating signal B. This pattern allows us to assign signals B and D as due to Hδ2 and Hϵ1 protons, respectively. The fact that these protons are not detectable at 600 MHz indicates that the Curie contribution[20,21] to the relaxation properties of these signals is rather significant. The assignment of the ring protons of the proximal histidine indicates that in the present protein the proximal histidine is coordinated via the NHϵ proton as usual.[37]

At this stage we are left with only one unassigned downfield signal (signal C) (Figure 1B). Its T_1 value (consistent with T_2) is substantially shorter (Table 1) than the T_1 values of other assigned heme protons in the α position. Therefore it corresponds to a proton close to the metal ion. The distance between this proton and the metal ion should be rather short and can be estimated to be 3−4 Å. Since no NOE on other assigned heme protons is observed, in the absence of information on the primary sequence this signal cannot be assigned at this stage, although it will be further discussed at the end of the next section.

All hyperfine shifted signals of the reduced cytochrome *c′* from *R. palustris* obey a Curie-type temperature dependence. A plot of the hyperfine chemical shifts against inverse temperature is shown in Figure 5. All signals under consideration reveal a large nonzero intercept at $T^{-1} = 0$. This probably reveals that both contact and pseudocontact interactions are operative. Another cause for this temperature dependence of the shifts is the splitting of the d_{xz}, d_{yz} orbital admixtures of a ^5E ground state[38,39] in rhombic symmetry (see later) which could be of the order of *kT* and would make two different levels accessible at room temperature. This is operative in low-spin ferric cytochromes.[40−43]

Discussion

In reduced cytochrome *c′* from both *R. palustris* and *R. gelatinosus* the shift pattern of the methyls is three signals upfield and one downfield. This is a rather unusual shift pattern which deserves attention. Since the X-ray structure is available for the latter protein, an attempt to account for the spectroscopic observation is here presented on the basis of the electronic structure.

Two 3d orbital schemes have been suggested for Fe^{2+}-containing heme proteins with an axial ligand (Scheme 1D,E).[38,39,44,45]

(37) Banci, L.; Bertini, I.; Bruschi, M.; Sompornpisut, P.; Turano, P. *Proc. Natl. Acad. Sci. U.S.A.* **1996**, *93*, 14396.
(38) Trautwein, A. X.; Zimmermann, R.; Harris, F. E. *Theor. Chim. Acta* **1975**, *37*, 89.
(39) Eaton, W. A.; Hanson, L. K.; Stephens, P. J.; Sutherland, J. C.; Dunn, J. B. R. *J. Am. Chem. Soc.* **1978**, *100*, 4991.
(40) Turner, D. L. *Eur. J. Biochem.* **1993**, *211*, 563.
(41) Turner, D. L. *Eur. J. Biochem.* **1995**, *227*, 829.
(42) Bertini, I.; Luchinat, C.; Macinai, R.; Martinuzzi, S.; Pierattelli, R.; Viezzoli, M. S. *Inorg. Chim. Acta* **1998**, *269*, 125.
(43) Shokhirev, N. V.; Walker, F. A. *J. Phys. Chem.* **1995**, *99*, 17795.
(44) La Mar, G. N.; Budd, D. L.; Goff, H. M. *Biochem. Biophys. Res. Commun.* **1977**, *77*, 104.

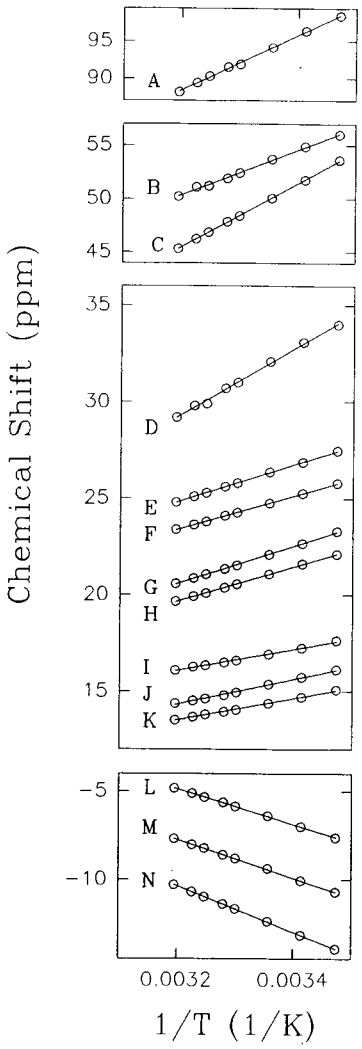

Figure 5. Experimental ^{1}H NMR temperature dependence of the hyperfine shifted signals of the reduced cytochrome *c*′ from *R. palustris* in 100 mM phosphate buffer water solution at pH 4.9.

In both schemes the $d_{x^2-y^2}$ provides σ spin delocalization and downfield contact shifts, in analogy with high spin Fe^{3+} heme systems[46] (Scheme 1A). All the methyls should have similar shifts. Unpaired electrons in the d_{z^2} and d_{xy} play a minor role for symmetry reasons. Only one unpaired electron in the d_{xz}, d_{yz} pair of orbitals (Scheme 1E) (or in a pair of combination of the two orbitals) provides large spreading of the contact shifts as observed in the case of low-spin iron(III) with the electronic structure of Scheme 1B, and introduces magnetic susceptibility anisotropy in the *xy* plane. This is what it is needed to account for the experimental data. In fact the d_{xz} and the d_{yz} orbitals contribute downfield contact shifts as in low-spin Fe^{3+} [47] (Scheme 1B,E). Pseudocontact shifts can shift the heme methyl protons upfield as it occurs in low spin Fe^{3+} heme systems.[48,49] According to eq 1,[50] the heme methyl protons should experience

$$\delta_{pc} = \frac{1}{12\pi r^3}\left[(3\cos^2\theta - 1)\left(\chi_{zz} - \frac{1}{2}(\chi_{xx} - \chi_{yy})\right) + \sin^2\theta \cos 2\Omega \frac{3}{2}(\chi_{xx} - \chi_{yy})\right] \quad (1)$$

upfield shift contributions if the axial ligand field strength is smaller than the equatorial one and therefore $\chi_{\parallel} > \chi_{\perp}$. So, depending on the relative weight of contact and pseudocontact contributions, the proton shifts should be upfield or downfield. The four methyl substituents can only be differentiated in a substantial manner by breaking the pseudo-4-fold symmetry of the heme moiety with an axial ligand introducing π interactions.

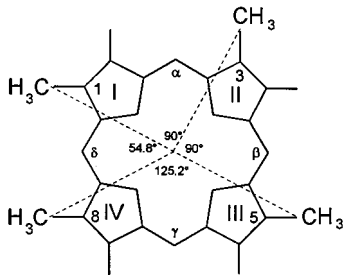

Figure 6. Schematic drawing of the heme moiety showing the geometric relationships among the four methyl group−iron ion directions.

The orientation of the χ axes in the porphyrin plane is known to depend on the orientation of the axial π interaction. When the π interaction axis rotates clockwise, the χ tensor axes rotate counterclockwise.[41,51−54] The pseudocontact shifts of the heme substituents (Figure 6) can be thus calculated as a function of the angle α defined by the orientation of the axial histidine as shown in Figure 7A, using the fixed geometric relationships between α and Ω in eq 1 for each heme group (see caption of Figure 7). The curves in Figure 7A are calculated assuming that (1) $\chi_{zz} > \chi_{xx}, \chi_{yy}$ and (2) that the χ component along the pyrrole−pyrrole axis along which the histidine ring plane lies for the starting $\alpha = 0$ value is the larger of the two. For simplicity, it has been further assumed that $\Delta\chi_{ax} = (3/2)\Delta\chi_{rh}$, and the extremal shift values have been normalized to −1. If the opposite assumption on the sign of $\Delta\chi_{rh}$ were made, all curves would be simply shifted by 90°. According to Figure 7A, a pattern of upfield shifts for methyls 1, 5, and 8 and a downfield shift for methyl 3 is obtained for a histidine orientation of 135°, i.e., along the $\beta-\delta$ meso axis. This orientation is what was found in the X-ray structure of cytochrome *c*′ from *C. vinosum*[26] and, more recently, in the X-ray structure of the cytochrome *c*′ from *R. gelatinosus*.[27] For the latter, the methyl assignment is also available, and the pattern is the same as that found in the present system. Therefore, the pseudocontact shift pattern would be in good agreement with the experimental data if the assumption on the sign of $\Delta\chi_{rh}$ is the one made in Figure 7A and not the opposite. This assumption has been verified by means of angular overlap calculations[55] (Figure 8), which under any conditions yield the smaller χ value along the pyrrole−pyrrole axis where the π interaction takes place (i.e., the larger χ value along the pyrrole−pyrrole axis contained in the histidine ring plane). Note that this behavior is analogous but opposite to what is expected and found in low-spin ferric cytochromes.[41,51,52] Angular overlap

(45) Banci, L.; Bertini, I.; Marconi, S.; Pierattelli, R. *Eur. J. Biochem.* **1993**, *215*, 431.
(46) La Mar, G. N.; Davis, N. L.; Johnson, R. D.; Smith, W. S.; Hauksson, J. B.; Budd, D. L.; Dalichow, F.; Langry, K. C.; Morris, I. K.; Smith, K. M. *J. Am. Chem. Soc.* **1993**, *115*, 3869.
(47) La Mar, G. N.; Walker, F. A. *J. Am. Chem. Soc.* **1973**, *95*, 1782.
(48) Horrocks, W. D., Jr.; Greenberg, E. S. *Biochim. Biophys. Acta* **1973**, *322*, 38.
(49) Trehwella, J.; Wright, P. E. *Biochim. Biophys. Acta* **1980**, *625*, 202.
(50) Kurland, R. J.; McGarvey, B. R. *J. Magn. Reson.* **1970**, *2*, 286.
(51) Oosterhuis, W. T.; Lang, G. *Phys. Rev.* **1969**, *178*, 439.
(52) Shulman, R. G.; Glarum, S. H.; Karplus, M. *J. Mol. Biol.* **1971**, *57*, 93−115.
(53) Banci, L.; Rosato, A.; Turano, P. *JBIC* **1996**, *1*, 364.
(54) Shokhirev, N. V.; Walker, F. A. *J. Am. Chem. Soc.*, in press.

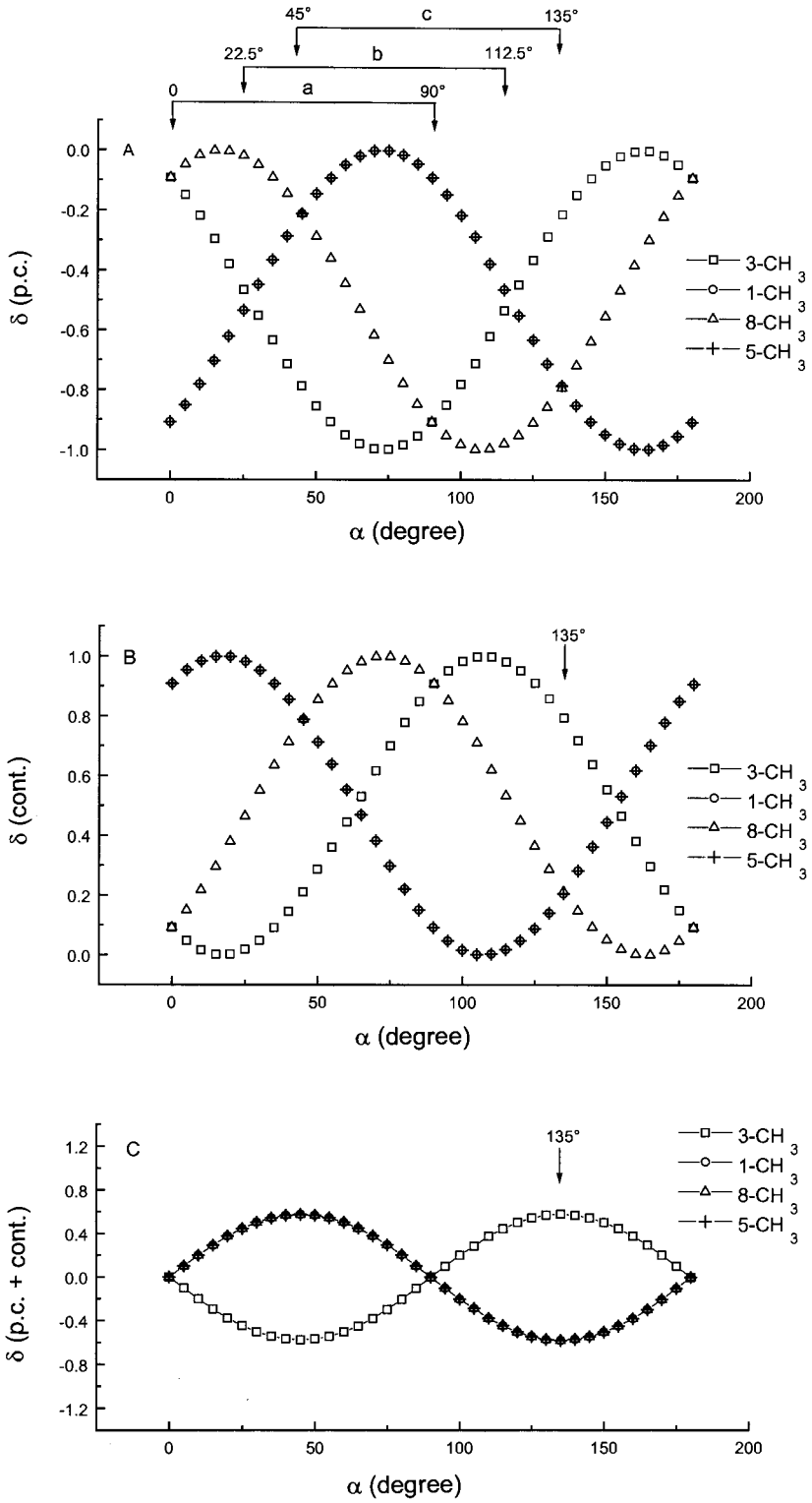

Figure 7. (A) Dependence of the heme methyl anisotropic part of the pseudocontact shifts as a function of the angle α between the pyrrole II−pyrrole IV molecular axis and the projection of the His plane on the heme. The Ω values for each methyl group are $\Omega_1 = \alpha + 17.6°$, $\Omega_3 = \alpha + 17.6° + 270°$, $\Omega_5 = \alpha + 17.6° + 180°$, and $\Omega_8 = \alpha - 17.6° + 90°$. Three different situations are pointed out: (a) the histidine is along the pyrrole II−IV axis ($\alpha = 0°$) or along pyrroles I−III ($\alpha = 90°$); (b) the histidine forms an angle α of 22.5° or 112.5° with the pyrrole II−IV axis; (c) the histidine is along the $\alpha-\gamma$ meso axis ($\alpha = 45°$) or along the $\beta-\delta$ meso axis ($\alpha = 135°$). (B) Dependence of the anisotropic part of the contact shift (π contribution) as a function of the same α. (C) Dependence of the sum of the anisotropic part of the pseudocontact plus contact shifts on the α angle. The sum is obtained giving the same weight to both contributions. All curves are reported on arbitrary scales.

calculations confirms that $\Delta\chi_{||} > \Delta\chi_{\perp}$ and justifies the counterclockwise rotation of the χ tensor *x* and *y* axes with respect to the imidazole plane.

The anisotropy of the contact shifts can be predicted to display the same dependence on the α angle as that shown by low-spin ferric cytochromes,[41,51,52,56] because the symmetry properties are the same, and this is depicted in Figure 7B. The contact shift is positive and maximal along the direction of the π interaction (i.e., perpendicular to the histidine ring plane) and zero at 90° from the direction of the π interaction (Figure 9). Again, a

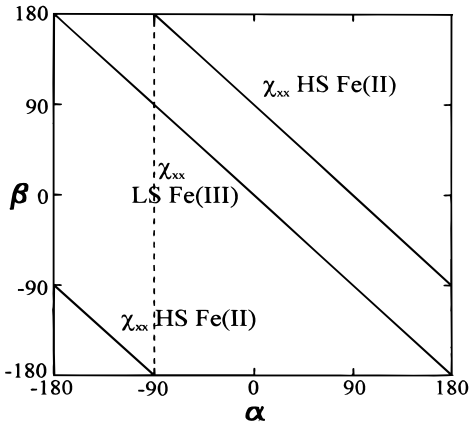

Figure 8. Orientation of the χ_{xx} axis of the pseudocontact tensor for Fe(III) low-spin and Fe(II) high-spin systems as a function of the orientation of the axial π interaction. The angles α for the π interaction and β for the χ_{xx} axis are defined relative to a pyrrole nitrogen−pyrrole nitrogen axis. These dependences have been obtained using angular overlap calculations and are independent of the angular overlap parameters as long as the orbital pattern of Scheme 1E (high-spin Fe(II)) or that of Scheme 1B (low-spin Fe(III)) holds. A typical set of angular overlap parameters is as follows: $e_\sigma = 4000\ cm^{-1}$, $e_{\pi y} = 500\ cm^{-1}$, $e_{\pi x} = 0$ for the heme moiety; $e_\sigma = 3000\ cm^{-1}$, $e_{\pi y} = 500\ cm^{-1}$, $e_{\pi x} = 0$ for the axial histidines.

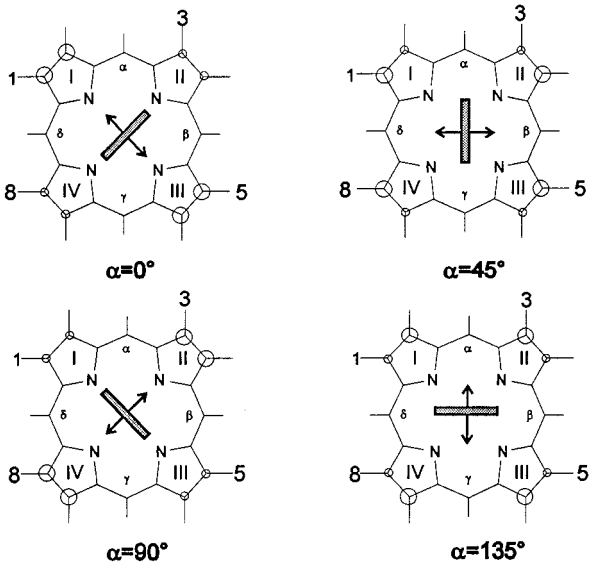

Figure 9. Angular dependence of the π interaction of the axial histidine with the porphyrin orbitals. Four different cases are pointed out. The π MO directions are indicated by two-headed arrows. The large and small circles give a qualitative picture of the spin densities in the β-pyrrole carbon p_z orbitals.

unitary extremal value of the shift is assumed. The predictions of Figure 7B are also in good agreement with the experimental data for $\alpha = 135°$. Therefore, it can be qualitatively concluded that both contact and pseudocontact shifts contribute to the in-plane hyperfine shifts of high-spin ferrous systems and in particular to the peculiar pattern observed in cytochromes c′. Indeed, the two contributions work in opposite directions, in such a way that the spreading between methyl 3, on one hand, and methyls 1, 5, and 8, on the other, is enhanced. This is illustrated in Figure 7C, where the sum of the two contributions, assumed equal, is shown.

At this point, a comment is due on the possibility that signal C is one of the unassigned heme protons, which, in principle, might be inconsistent with the above picture. Since, as mentioned in the Results, carefully performed[33,34] 1D NOE experiments on signal C do not show a NOE on any assigned heme proton, signal C cannot belong to a meso proton (which would have given a NOE on either methyl(s) or propionate Cα(s)) nor to the CH of thioether 4 which should have given a NOE to methyl 4. Of course, checks have been performed, based on heme T_1's, that such NOEs would have been largely above the signal-to-noise threshold of the experiment. We feel that signal C cannot be attributed to the CH of thioether 2 for a series of clues; however, even if it were, a large downfield shift would be consistent with our theoretical picture. A proton from a protein side chain in the axial position on the opposite side of the coordinated histidine would be expected to experience a large downfield pseudocontact shift. At least one proton as close as 3−4 Å is present in all X-ray structures of cytochrome *c*′.[23,27,57,58]

Concluding Remarks and Considerations on Analogous Systems

NMR techniques tailored to the detection of the proton−proton dipolar connectivities between fast relaxing protons have allowed us to perform an extensive assignment of the protons of the heme and of the coordinated histidine in a high-spin Fe^{2+} system. The observed shift pattern with the 1-, 5-, and 8-methyl signals upfield and the 3-methyl signal downfield both for the present system and for the reduced cytochrome *c*′ from *R. gelatinosus*[30] is semiquantitatively ascribed to a particular orientation of the histidine plane. In fact if the imidazole plane is along the $\beta-\delta$ meso protons, analogy with low-spin Fe^{3+} systems allows us to account for the experimental data on the basis of both the pseudocontact shift and contact shift contributions.

Despite the unavailability of the assignment of the reduced cytochrome *c*′ from *Chromatium vinosum*, the similarity of the structure leads to the same assignment,[59] the available X-ray structure[26] being consistent with the model here discussed (Table 2). The same conclusion can be proposed for the cytochrome *c*′ from *Rhodospirillum rubrum* on the basis of the ^{1}H NMR spectra although neither the assignment nor the X-ray structure is available (Table 2).

The analysis can be extended to deoxyhemoglobins. In the protein from *Aplysia limacina* the pattern of the shifts[60] is similar to that found in cytochromes *c*′, and indeed the histidine plane is relatively close (15°) to the $\beta-\delta$ meso axis.[61] This is a further proof of the validity of the present criterion.

In the case of deoxymyoglobin from sperm whale (Table 2),[45,46] the position of the histidine along the pyrrole II−pyrrole

(55) Angular overlap calculations were performed using a modified version of the program CAMMAG (Cruse, D. A.; Davies, J. E.; Harding, J. H.; Macking, D. J.; McMeeking, R. F. *CAMMAG, A Fortran computing package*; University Chemical Laboratory: Cambridge, England, 1979). The calculation procedure was similar to that described in ref 53. The ligand field parameters for the nitrogen of the heme and of the axial histidine were varied within a relatively large range of values to obtain a range of χ anisotropy values and orientation of the χ tensor.

(56) Walker, F. A.; Buehler, J.; West, J. T.; Hinds, J. L. *J. Am. Chem. Soc.* **1983**, *105*, 6923.

(57) Tahirov, T. H.; Misaki, S.; Meyer, T. E.; Cusanovich, M. A.; Higuchi, Y.; Yasuoka, N. *J. Mol. Biol.* **1996**, *259*, 467.

(58) McRee, D. E.; Redford, S. M.; Meyer, T. E.; Cusanovich, M. A. *J. Biol. Chem.* **1990**, *265*, 5364.

(59) Bertini, I.; Briganti, F.; Monnanni, R.; Scozzafava, A.; Carlozzi, P.; Materassi, R. *Arch. Biochem. Biophys.* **1990**, *282*, 84.

(60) Wüthrich, K.; Hochmann, J.; Keller, R. M.; Wagner, G.; Brunori, M.; Giacometti, C. *J. Magn. Reson.* **1975**, *19*, 111.

(61) Bolognesi M.; Onesti, S.; Gatti, G.; Coda, A.; Ascenzi, P.; Brunori, M. *J. Mol. Biol.* **1989**, *205*, 529.

Table 2. Summary of the ^{1}H NMR Assignment of Heme Methyl Substituents and Proximal Histidine Ring Protons for the Investigated Proteins Containing High-Spin Iron(II)

protein	NMR pattern of heme methyls	NMR pattern of proximal histidine	refs
reduced cyt *c*′ from *R. gelatinosus*	1-CH_3 = upfield 3-CH_3 = downfield 5-CH_3 = upfield 8-CH_3 = upfield	not reported	30
reduced cyt *c*′ from *R. palustris*[a]	1-CH_3 = upfield: −6.38 ppm 3-CH_3 = downfield: 22.10 ppm 5-CH_3 = upfield: −12.36 ppm 8-CH_3 = upfield: −9.38 ppm	NHδ1 = 93.74 ppm Hδ2 = 53.73 ppm Hϵ1 = 32.01 ppm	this work
reduced cyt *c*′ from *C. vinosum*[b]	1-CH_3 = upfield 3-CH_3 = downfield 5-CH_3 = upfield 8-CH_3 = upfield	NHδ1 = 104.00 ppm	59
reduced cyt *c*′ from *R. rubrum*[b]	1-CH_3 = upfield 3-CH_3 = downfield 5-CH_3 = upfield 8-CH_3 = upfield	NHδ1 = 93.00 ppm Hδ2 or Hϵ1 = 33.00 ppm	64, 65
reduced deoxy-Mb from sperm whale[c]	1-CH_3 = downfield: 7.7 ppm 3-CH_3 = downfield: 10.9 ppm 5-CH_3 = downfield: 15.8 ppm 8-CH_3 = downfield: 7.7 ppm	NHδ1 = 75.2 ppm Hδ2 = 42.2 ppm Hϵ1 = 42.2 ppm	63 63
reduced deoxy-Mb from *Aplysia limacina*	three CH_3 signals are upfield, and one is downfield	not reported	60

[a] Shifts are measured at 298 K. [b] Assignment of the heme methyl signals is not available. We propose the assignment on the basis of the similarity of the NMR pattern to the NMR patterns of the reduced cytochromes *c*′ from *R. gelatinosus* and *R. palustris.* [c] Shifts are measured at 308 K.

IV axis (the histidine plane is misaligned with the axis by only 6°)[62] causes the rhombic pseudocontact and π contact interactions to play opposite roles, to the extent that they may largely cancel each other (Figure 7C for α close to 0°). A factorization recently proposed in the literature[63] indicates that methyls 1 and 5 experience upfield pseudocontact shifts whereas methyls 3 and 8 experience downfield ones, in agreement with Figure 7A. The calculated contact shifts are larger (7.16 and 15.7 ppm) for protons 1 and 5 than for protons 3 and 8 (4.95 and 3.50 ppm), again in qualitative agreeement with Figure 7B. This scheme considers only π delocalization, whereas some σ contribution may be present, which would shift all methyl protons downfield, as observed.[45,46]

Acknowledgment. This work is partially supported by MURST "Cofinanziamento programmi di interesse nazionale—ex 40%" 1997, "Progetto Finalizzato Biotecnologie", "Comitato Biotecnologie", "Comitato Scienze Agrarie", and "Comitato Nazionale Scienze Tecnologie dell'Ambiente e Habitat" of CNR, Italy, by Human Capital and Mobility Program, Network "Structure−function relationship in iron−sulfur proteins", No. ERBCHRXCT 040626, INTAS Project 94-552, and by CEE Contract CHRX-CT94-0540.

IC980531C

(62) Yang, F.; Phillips, G. N. J. *J. Mol. Biol.* **1996**, *256*, 762.
(63) Bougault, C. M.; Dou, Y.; Ikeda-Saito, M.; Langry, K. C.; Smith, K. M.; La Mar, G. N. *J. Am. Chem. Soc.* **1998**, *120*, 2113−2123.
(64) Emptage, M. H.; Xavier, A. V.; Wood, J. M.; Alsaadi, B. M.; Moore, G. M.; Pitt, R. C.; Williams, R. J. P.; Ambler, R. P.; Bartsch, R. G. *Biochemistry* **1981**, *20*, 58.
(65) La Mar, G. N.; Jackson, J. T.; Bartsch, R. G. *J. Am. Chem. Soc.* **1981**, *103*, 4405.